Double Quantum NMR Applied to Polymer Networks with Low Concentration of Pendant Chains

Rodolfo H. Acosta,[†] Daniel A. Vega,[‡] Marcelo A. Villar,[§] Gustavo A. Monti,*[,†] and Enrique M. Vallés[§]

LANAIS RMS-Fa.M.A.F, Universidad Nacional de Córdoba-CONICET, Medina Allende s/n, Ciudad Universitaria, 5016 Córdoba, Argentina; Department of Physics, Universidad Nacional del Sur-CONICET, Av. L. N. Alem 1253, 8000 Bahía Blanca, Argentina; and Planta Piloto de Ingeniería Química, PLAPIQUI (UNS-CONICET), Camino La Carrindanga Km 7, CC717, 8000 Bahía Blanca, Argentina

Received January 3, 2006; Revised Manuscript Received May 15, 2006

ABSTRACT: The influence of pendant chains at low concentrations in poly(dimethylsiloxane) networks is studied using double quantum proton nuclear magnetic resonance. Small relative variations of the average molecular weight of the elastically active chains, the molecular weight of pendant chains, and the concentration of pendant chains were analyzed. Changes induced by these defects in the residual dipolar couplings are related to changes in the viscoelastic relaxation times and compared against the behavior of the elastic shear modulus. A very good correlation between NMR measurements and the corresponding rheological experiments is found.

1. Introduction

The mechanical response of polymeric materials is strongly correlated to its structure. In the particular case of polymer networks, chemical or physical cross-linking points give distinctive characteristics to these materials such as high elastic elongation, good thermal stability, and insolubility. Model silicone networks have been extensively studied in order to explain the influence of molecular structure on mechanical properties. Free chains (solubles) and pendant chains are the more common defects in polymer networks. Figure 1 is a schematic representation of a network where defects, such as free and dangling chains, are shown. The relative concentration and molecular structure of these defects have a strong influence on the viscoelastic properties of networks, changing considerably the spectrum of relaxation times. However, there are few works in which the influence of network defects on the nonequilibrium properties were investigated.[1,2] Most of the studies concerning pendant chains have been focused on polymer networks obtained by random cross-linking reactions.[3] However, in those networks, little is known about the structure of the dangling chains, such as their molecular weight, molecular weight distribution, degree of branching, etc. Recently, we have synthesized model PDMS networks with controlled amounts of well-characterized pendant chains, which constitute an ideal system to reveal the basic mechanisms responsible for structural behaviors of more complex systems.[4−7] Networks with controlled amounts of well-characterized defects are particularly suitable system to reveal the effects of defects on the structure of networks. In addition, model networks have proved to be very useful to elucidate the basic mechanism of relaxation in polymers with branched structures.[8]

NMR techniques are commonly used to unravel the fundamental properties of polymers.[9,10] For cross-linked elastomers above the glass transition temperature, NMR provides information on the structure and dynamics of the polymer chains in the bulk.[11−17] Several ^{1}H NMR experiments like transverse ^{1}H relaxation (Hahn spin echoes),[11−13] pseudo-solid spin echoes,[15] 2D-exchange experiments,[16] and multiple quantum (MQ) coherence excitation,[17,18] have been used to probe different aspects of the structure and dynamics of polymer chains at the molecular level.

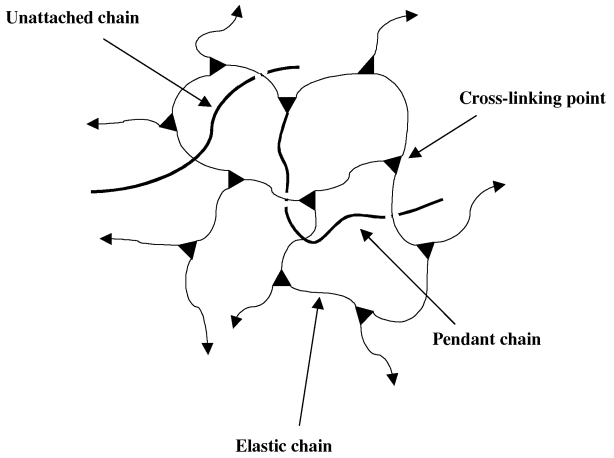

Figure 1. Schematic representation of the network structure. Arrows indicate connection to the gel.

Proton residual dipolar interactions measured by NMR provide information about the structure and molecular dynamics in soft solids like elastomers. Therefore, changes in the structure (cross-linking density, the presence of fillers, the action of mechanical deformation forces, and other network defects) and their influence on the dynamic response can be investigated via changes induced in the residual dipolar couplings. One approach to model-free access to the residual dipolar couplings and dynamical order parameters uses MQ buildup curves (Voda et al. and references therein)[18] recorded in the initial regime of the excitation/reconversion periods. It has been shown that the relevant quantity for analysis of double-quantum (DQ) buildup curves in the initial regime is the second van Vleck moment.[18]

[†] Universidad Nacional de Córdoba-CONICET.
[‡] Universidad Nacional del Sur-CONICET.
[§] PLAPIQUI (UNS-CONICET).
* Corresponding author: Tel +54-351-4334051; Fax +54-351-4334054; e-mail monti@famaf.unc.edu.ar.

10.1021/ma060011y CCC: $33.50
Published on Web 06/15/2006

Table 1. Nomenclature Used, Bifunctional Molecular Weight (Mw_{B2}), Monofunctional Molecular Weight (Mw_{B1}), Weight Fraction of Monofunctional Chains (w_{B1}), Extent of Reaction (p_∞), and Fraction of Pendant Chains (W_p) As Determined from NMR Transverse Relaxation Measurements

network	Mw_{B2} (g/mol)	Mw_{B1} (g/mol)	w_{B1}	W_s (g/g)	p_∞	W_p
$B_{2,1}$-00	21 500			0.004	0.954	0.117
$B_{2,1}$-$B_{1,5}$-01	21 500	121 300	0.013	0.004	0.938	0.084
$B_{2,1}$-$B_{1,5}$-05	21 500	121 300	0.049	0.007	0.940	0.092
$B_{2,1}$-$B_{1,5}$-10	21 500	121 300	0.097	0.011	0.943	0.108
$B_{2,1}$-$B_{1,5}$-15	21 500	121 300	0.146	0.016	0.939	0.121
$B_{2,1}$-$B_{1,5}$-20	21 500	121 300	0.195	0.023	0.932	0.140
$B_{2,2}$-00	23 900			0.007	0.937	0.111[a]
$B_{2,2}$-$B_{1,1}$-20	23 900	26 500	0.202	0.049	0.906	0.322[a]
$B_{2,2}$-$B_{1,2}$-20	23 900	51 300	0.201	0.043	0.906	0.220[a]
$B_{2,2}$-$B_{1,3}$-20	23 900	60 600	0.199	0.041	0.880	0.188[a]
$B_{2,2}$-$B_{1,4}$-20	23 900	83 500	0.201	0.039	0.892	0.178[a]
$B_{2,2}$-$B_{1,5}$-20	23 900	121 300	0.199	0.039	0.896	0.182[a]
$B_{2,3}$-$B_{1,5}$-10	11 900	121 300	0.096	0.001	0.996	0.100

[a] From ref 6.

In earlier works this technique was applied to investigate the behavior of specially prepared elastomers[18] with different degree of cross-linking or in model networks[19,20] with small contents of dangling chains arising from incomplete reaction of precursor chains. On the other hand, in a recent publication the second van Vleck moment has been shown to scale with a polynomial dependence on shear modulus.[21]

In this work we tested the sensitivity of DQ NMR to detect the influence of network defects on model polymer networks with a controlled amount of pendant chains. DQ NMR experimental data are widely and very well correlated with those data obtained by rheological techniques[5,6] from model networks containing elastic and pendant chains of different molecular weights and various concentrations of pendant chains.

2. Materials and Methods

2.1. Molecular Structure. Preparation and characterization of the polymer networks used here have been reported in detail by Vega et al.[6] and Roth et al.[7] Model poly(dimethylsiloxane) networks were obtained by the hydrosylilation reaction, based on the addition of hydrogen silanes from the cross-linker molecules to the end vinyl groups present in the prepolymer molecules. A commercial difunctional prepolymer, α,ω-divinylpoly(dimethylsiloxane) (B_2) (United Chemical Technology, Inc.), and several monodisperse monofunctional prepolymers, ω-vinylpoly(dimethylsiloxane) (B_1), were used to generate the elastic and pendant chains of the model networks, respectively. Phenyltris(dimethylsiloxy)silane (A_3) was used as cross-linker, and a Pt salt was employed as catalyst. The monofunctional prepolymer was synthesized by anionic polymerization of hexamethylcyclotrisiloxane. The reaction was carried out on a conventional glass reactor utilizing *n*-butyllithium as initiator, *n*-hexane as solvent, and tetrahydrofuran as promoting agent. Number- and weight-average molecular weights were obtained by measuring the concentration of end groups by infrared (FTIR) and by size exclusion chromatography (SEC) (see Table 1 and ref 7 for more details).

Networks prepared with low amounts of monofunctional chains in stoichiometrically balanced systems contain almost exclusively linear pendant chains with the same molecular weight than the monofunctional chains added to the initial reaction mixture. To keep the probability of obtaining more complex branched pendant chains low, the concentration of monofunctional chains added to the initial formulation was kept, in this work, lower than 20 wt %.[4,5,7] The notation employed to identify the different networks is $B_{2,i}$-$B_{1,j}$-*XX*. $B_{2,i}$ with $i = 1-3$ identifies the three bifunctional end-linked PDMS that generate the elastic chains, with molecular weights of 21 500, 23 900, and 11 900 g/mol, respectively. $B_{1,j}$ with $j = 1-5$ categorizes the monofunctional prepolymers employed to make the pendant chains with molecular weights of 26 500, 51 300, 60 600, 83 500, and 121 300 g/mol. Finally, the last number, *XX*, indicates the weight fraction of monofunctional chain employed in the formulation of each network. Table 1 shows the molecular weights of the different network precursors.

Table 2. Elastic Modulus ($G'_{\omega=1000}$), Second Van Vleck Moment $(M_2)^{1/2}$, and Apparent T_2^* Obtained from the Fitting of Eq 2

network	$G'_{\omega=1000}$ (MPa)	$(M_2)^{1/2}$ (2πkHz)	T_2^* (ms)
$B_{2,1}$-00	0.270	1.66	1.3
$B_{2,1}$-$B_{1,5}$-01	0.257	1.65	1.3
$B_{2,1}$-$B_{1,5}$-05	0.249	1.61	1.3
$B_{2,1}$-$B_{1,5}$-10	0.245	1.50	1.4
$B_{2,1}$-$B_{1,5}$-15	0.243	1.44	1.4
$B_{2,1}$-$B_{1,5}$-20	0.230	1.40	1.4
$B_{2,2}$-00	0.216	1.43	1.5
$B_{2,2}$-$B_{1,1}$-20	0.122	1.06	2.3
$B_{2,2}$-$B_{1,2}$-20	0.150	1.28	1.6
$B_{2,2}$-$B_{1,3}$-20	0.164	1.37	1.5
$B_{2,2}$-$B_{1,4}$-20	0.164	1.25	1.7
$B_{2,2}$-$B_{1,5}$-20	0.178	1.32	1.6
$B_{2,3}$-$B_{1,5}$-10	0.330	1.80	1.1

2.2. Elastic Modulus. Viscoelastic measurements were done on a dynamic rotational rheometer, Dynamic Analyzer RDA II (Rheometrics), between parallel plates of 25 mm diameter under a nitrogen atmosphere. The oscillation frequency ranged from 0.05 to 500 s^{-1}, and the temperature in the environmental chamber was varied between 243 and 473 K. Time−temperature superposition allowed to extend the frequency range to the region of frequencies reported in this work ($\omega = 1000\ s^{-1}$). The shifting factors for the time−temperature superposition were in good agreement with results previously reported for PDMS networks.[4] Following extraction, samples were weighed and dried under vacuum at 313 K until complete solvent removal was achieved. Table 2 shows the experimentally measured elastic modulus at a frequency of 1000 s^{-1} ($G'_{\omega=1000}$) at a reference temperature of 273 K.

Shear equilibrium modulus can be calculated from the elastic modulus in the limit at low frequencies ($G'_{\omega\to 0}$). Theoretical predictions of this modulus can be obtained on the basis of the theory of elasticity, taking into account the contribution of molecular entanglements[22,23] as

$$G'_{\omega\to 0} = (\nu - h\mu)RT + G_e T_e \qquad (1)$$

where ν is the concentration of elastically active chains, h an empirical constant (taking values from 0 to 1), μ the concentration of cross-linking points, R the gas constant, and T the absolute temperature. T_e is the fraction of trapped entanglements in the network, and G_e is the maximum contribution to the modulus due to trapped entanglements. Since both the elastic modulus at low frequencies and the relaxation modulus at long times are a measure of the energy stored during the deformation, they will be equal to the shear equilibrium modulus. At high frequencies the entanglements involving pendant chains are not able to relax, and they behave as elastic chains, acting then as additional cross-linking points.[4,8]

2.3. Residual Dipolar Couplings. NMR measurements presented in this work were performed in a Bruker MSL300 spectrometer operating at a resonance frequency of 300.13 MHz for protons. A DOTY DSI-703 proton dedicated probe with proton background signal reduction was used. Samples were packed in 4 mm o.d. ZrO sample holders fitted with Kel-F end-caps. All NMR measurements were carried out at a temperature of 302 K. After viscoelastic measurements, networks were subjected to extraction of solubles using toluene as solvent. For this purpose, samples were placed in jars containing solvent to remove non-cross-linked polymer chains, for at least 1 month at room temperature until constant weight was achieved. Solvent was replaced every 3−4 days. This procedure was proved to be appropriate for complete extraction of the soluble fraction.

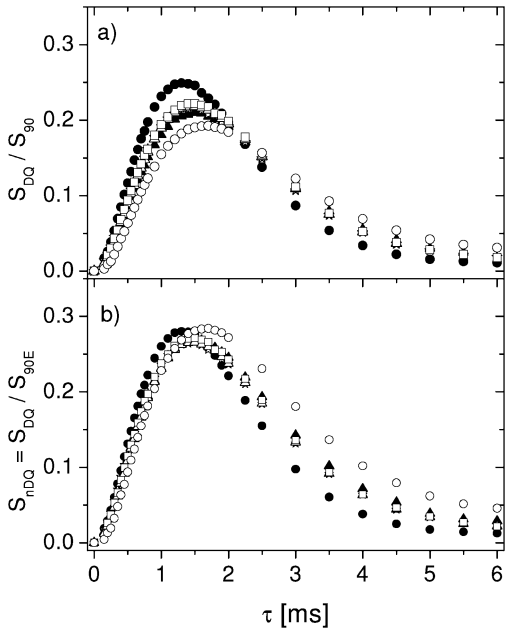

Figure 2. (a) DQ signal normalized to the full FID. (b) DQ signal normalized to the contribution of the elastic chains to the FID. Symbols correspond to the networks: (●) $B_{2,2}$-00, (▲) $B_{2,2}$-$B_{1,1}$-20, (☆) $B_{2,2}$-$B_{1,2}$-20, (△) $B_{2,2}$-$B_{1,3}$-20, (□) $B_{2,2}$-$B_{1,4}$-20, and (○) $B_{2,2}$-$B_{1,5}$-20.

Even-order MQ coherences, in a spin system initially polarized in the static magnetic field, were created using a five-pulse sequence with refocusing 180° pulses [$90°_{x+\Delta\phi}-\tau/2-180°-\tau/2-90°_{-x+\Delta\phi}-t_1-90°_y-\tau/2-180°-\tau/2-90°_y-t_f-90°_x$].[18,24] The first two 90° pulses excite even-order MQ coherences that are reconverted to *z*-polarization, after a short evolution time t_1, by means of the second 90° pulse pair. The NMR signal is obtained by means of a 90° pulse applied after a time t_f. Steps of $\Delta\phi = \pi/2$ were used for MQ coherence selection. The phases of the 180° pulses follow the pattern $0,\pi/2$ for the excitation period and $\pi/2,\pi$ for the reconversion period and were selected empirically to maximize the MQ signals. It is worth mentioning that the use of refocusing pulses leads to a better performance of the sequence for the investigated samples. The receiver phase was cycled in $\pm\pi$ on each acquisition in order to remove undesired coherences. The evolution time t_1 was set to 20 μs and the *z*-filter, t_f, to 8 ms, which is ∼5 times the effective transverse relaxation time T_2^*.

It has been shown that for excitation times much shorter than the effective transverse relaxation time ($\tau \ll T_2^*$) only DQ coherences are detected.[18] As excitation/reconversion time increases, DQ multispin correlations are present as well as high-order MQ coherences of $4n + 2$ order, with n an integer. Nevertheless, for soft solidlike elastomers and small values of τ, the DQ buildup curve follows the expression

$$S_{DQ}(2\tau) = \left(\frac{M_2}{2}\tau^2\right)\exp\left[-\frac{2\tau}{T^*_2}\right] \qquad (2)$$

where M_2 is the second van Vleck moment.

2.3.1. Normalization of DQ Buildup Curves. From eq 2 it becomes clear that the prefactor to the parabolic initial rise contains the information on the residual dipolar couplings. To obtain an absolute value for the dipole−dipole coupling strengths, extreme care must be taken in the definition of 100% scale of the DQ intensity. Figure 2a shows the intensity of the DQ signals, S_{DQ}, of the $B_{2,2}$-$B_{1,i}$-20 networks as a function of τ normalized to the intensity of the signal obtained after a single 90° pulse, S_{90}. As is well-known, NMR signal decay from elastomers can be described as the sum of two contributions. These are the contributions of the elastically active chains (solidlike behavior), on one hand, and dangling chains (liquidlike), on the other.[12] The dangling chains, or at least their unentangled part, appear isotropically mobile in NMR experiments and thus do not contribute to the DQ signal. They, however, do contribute to the overall NMR signal, and thus, the fitting results to the DQ buildup curves would depend on their proportion unless they are properly accounted for. We have determined the fraction of the two contributions from Hahn spin-echo experiments as described in ref 6. The fraction of pendant chains, W_p, is shown in Table 1 for all the networks. The DQ signals are then obtained by a normalization with respect to the contribution of the elastic chains to the FID, $S_{90E} = S_{90}(1 - W_p)$, i.e., $S_{nDQ} = S_{DQ}/S_{90E}$. Figure 2b shows the appropriately normalized DQ signals $S_{nDQ}(\tau)$.

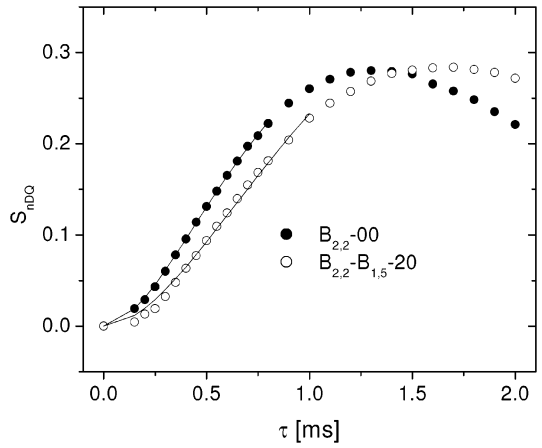

Figure 3. Normalized DQ signal as a function of time. Symbols: (●) $B_{2,2}$-00 network and (○) $B_{2,2}$-$B_{1,5}$-20 network. Solid lines are fittings of eq 1 to the data and yield M_2 values of $2.05 \times 4\pi^2\text{kHz}^2$ and $1.74 \times 4\pi^2\text{kHz}^2$, respectively.

2.3.2. Determination of Residual Dipolar Couplings. Figure 3 shows buildup curves for the networks $B_{2,2}$-00 and $B_{2,2}$-$B_{1,5}$-20. In this figure the solid lines correspond to the fittings of the experimental data with eq 2. Data were fitted up to a value of 80% of the individual buildup curves; this choice was made taking into account both the constraint $\tau \ll T_2^*$, necessary for the validity of eq 2, and the output of well-defined fitting parameters. Fittings between 40 and 80% of the buildup curve maxima result in deviations of less than 10% in the M_2 values. The values of $(M_2)^{1/2}$ thus obtained are listed in Table 2.

2.4. Relationship between the Residual Second van Vleck Moment and the Elastic Modulus. Following the work of Cohen-Addad,[25] it can be shown that the dependence of the residual second van Vleck moment on cross-linking density is described by the following equation

$$\langle M_2\rangle \sim \frac{3}{5}\frac{1}{N^2} \qquad (3)$$

where N is the effective number of statistical segments which, on a microscopic scale, represents the average chain length between both chemical and physical cross-links.[14] If we assume a linear dependence of G with $1/N$, as is the case of an ideal polymer networks, a linear dependence of G with $(M_2)^{1/2}$ is expected.

3. Results and Discussion

3.1. Concentration of Defects. The elastic modulus decreases with an increase in the concentration of pendant chains (w_{B1}) due to the drop in the concentration of elastically active chains per unit volume (ν). In the limit of low frequencies this behavior is well described by eq 1.[4,7] Figure 4 shows the $G'_{\omega=1000}$ values[6,7] as a function of the concentration of pendant chains for a fixed molecular weight ($Mw_{B1} = 121\,300$ g/mol) and three different values of the molecular weight of the elastically active chains. Data represented by triangles correspond to networks with an intermediate value of the elastically active chains ($Mw_{B2} = 21\,500$ g/mol).

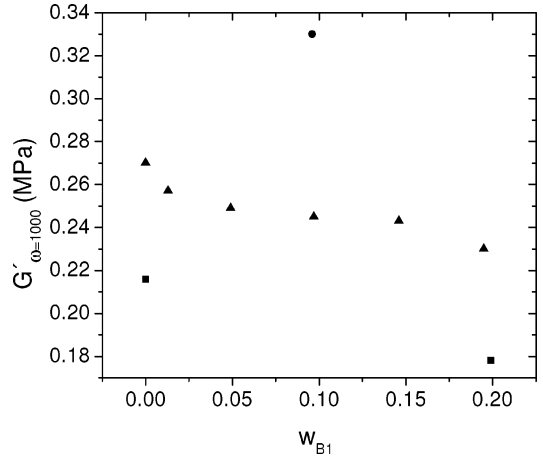

Figure 4. $G'_{\omega=1000}$ values as a function of weight fraction of monofunctional chains (w_{B1}) obtained from refs 3 and 6. Symbols: (●) $B_{2,1}$ network, (▲) $B_{2,2}$ networks, and (■) $B_{2,3}$ networks.

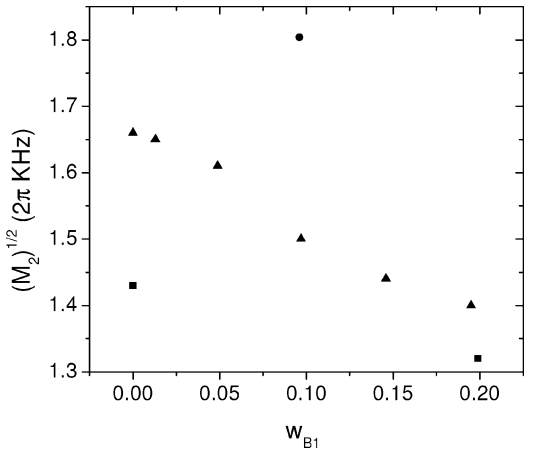

Figure 5. $(M_2)^{1/2}$ values, obtained by fitting eq 2, as a function of weight fraction of monofunctional chains (w_{B1}) for three different difunctional chain molecular weights (symbols: (●) $B_{2,1}$ network, (▲) $B_{2,2}$ networks, and (■) $B_{2,3}$ networks).

The same networks analyzed by DQ NMR (triangles in Figure 5) show an analogous dependence of $(M_2)^{1/2}$ with the concentration of pendant chains for networks prepared with the three different molecular weight of difunctional chains.

The elastic moduli as well as the residual dipolar couplings present a reduction of about 15% when a 20 wt % of monofunctional chains are added. The reduction of the second moment is also due to the drop in the concentration of elastically active chains per unit volume that decreases with increasing amounts of pendant chains. The experimental results clearly show that this larger amount of pendant chains produce a higher motional average of the dipolar interaction. On the other hand, a drop in the concentration of elastically active chains corresponds to a decrease in the concentration of cross-linking points. In Figure 6, the behavior of $G'_{\omega=1000}$ vs $(M_2)^{1/2}$ is shown. A linear relation is observed as is expected according to the model outlined in section 2.4. The small departures of the data from the linearity can be attributed to small differences in the extent of reaction of the different networks.[4]

Note that in order to better compare the data of rheology and DQ NMR we have considered the shear storage modulus at high frequencies instead of the equilibrium modulus. Since the time window of the DQ NMR experiments is in the range of a few milliseconds, it appears to be reasonably to correlate both measurements at a similar time scale. However, because of the fact that the additional contribution to the elastic modulus

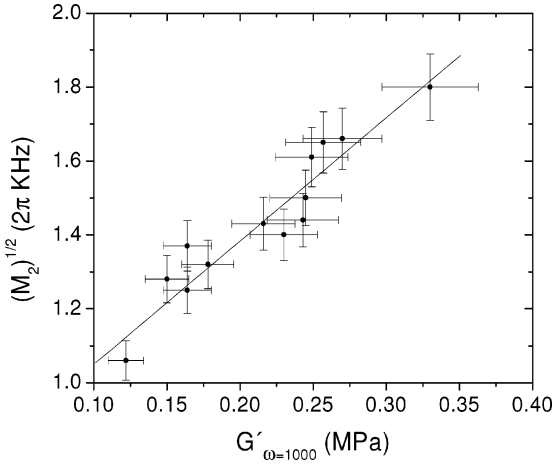

Figure 6. $(M_2)^{1/2}$ as a function of the elastic modulus ($G'_{\omega=1000}$) for all the networks.

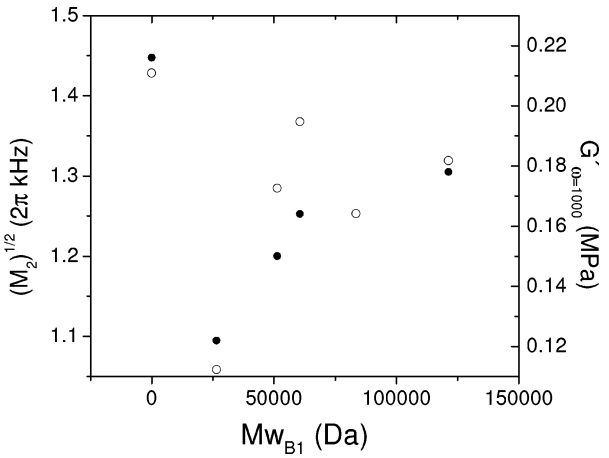

Figure 7. $(M_2)^{1/2}$ (○) and $G'_{\omega\to1000}$ (●) as a function of the weight-average molecular weight of monofunctional chains added (Mw_{B1}).

of the entangled pendant chains is not very high, we found similar results when $(M_2)^{1/2}$ is compared with the equilibrium shear modulus.

3.2. Pendant Chain Molecular Weight Dependence. When the experimental maximum extent of reaction (p_∞) of a stoichiometrically balanced formulation is close to unity, pendant chains are mostly linear molecules connected to the network by one end.[3] Maximum extent of reaction was calculated from the weight fraction of soluble material, W_s, using the recursive method[5] (Table 1). In this work maximum extents of reaction were estimated from calculations of the measured fraction of solubles as reported in the fifth column of Table 1. On the other hand, physical entanglements involving pendant chains are produced when the weight-average of pendant chains is higher than the weight-average molecular weight between entanglements. Depending on network structure, the average molecular weight between entanglements is determined by the molecular weight between cross-linking points or the molecular weight between entanglements in the melt.[26] At high frequencies of deformation these topological interactions behave like physical cross-links contributing to the elastic response of the network.[4]

To verify the influence of entanglements on structural properties, the length of monofunctional chains added to the $B_{2,2}$ network was changed using $B_{2,2}$ as difunctional chains. Figure 7 reports the elastic modulus at 1000 s^{-1} (filled circles) and $(M_2)^{1/2}$ values (open circles) obtained for networks with a fixed weight fraction (20 wt %) of pendant chains of different molecular weights. As pendant chains used in this work are

above the average molecular weight between entanglements M_e for linear PDMS melts, which is of the order of 9800 g/mol,[27] and the critical molecular weight in order to obtain a temporary network in a dynamic measurement is between 2 and 3 times M_e, a definite contribution to the elastic response of the pendant chains is expected. The network without monofunctional chains ($w_{B1} = 0$) is included for comparison. Upon addition of pendant chains with low molecular weight a drastic drop in the residual dipolar coupling is observed with respect to the network without pendant chains. This behavior is expected due to a decrease in the concentration of the elastically active chains, as explained in section 3.1. As the length of the pendant chains increases, the values of $(M_2)^{1/2}$ increase correspondingly and then level off to an average value of ca. $1.3 \times 2\pi$kHz as Mw_{B1} is further increased. The initial increment of $(M_2)^{1/2}$ is related to the presence of entanglements in the pendant chains. As mentioned above, the critical molecular weight necessary to obtain a temporary network in a dynamic measurement is between 20 000 and 30 000 g/mol; correspondingly, the effects of entanglements on the polymer network upon addition of pendant chains are expected for pendant chains with molecular weight higher than these values. Figure 7 shows that this behavior is reflected by the elastic modulus as well as the $(M_2)^{1/2}$ dependence on Mw_{B1}.

3.3. Elastically Active Chains Molecular Weight Dependence. Data represented by squares ($B_{2,2}$-00 and $B_{2,2}$-$B_{1,5}$-20) and circles ($B_{2,3}$-$B_{1,5}$-10) in Figures 4 and 5 correspond to measurements of elastic modulus and $(M_2)^{1/2}$, respectively, for networks with different molecular weight of the difunctional prepolymers (Mw_{B2}). It can be observed from these values that, independently of the pendant chain concentration, the structural variation of elastically active chains results in dynamic changes of the network. Increasing the molecular weight of the elastically active chains produces an increase in the mean distance between cross-linking points, resulting in a softer network structure. On the other hand, a decrease of Mw_{B2} will result in a more rigid structure as depicted by the increase in elastic modulus and residual dipolar couplings. Finally, it can be observed that DQ NMR seems to be as sensitive as rheological measurements are to small changes of the density of elastically active chains in the network structure.

3.4. Transverse Relaxation Times. The apparent transverse relaxation times T_2^* obtained by fitting of eq 2 are shown in the last column of Table 2. By a direct comparison with the obtained $M_2^{1/2}$ values a change in the dynamics upon the variation of the networks by the introduction of chains, both monofunctional and difunctional, with different molecular weights is observed. This effect is very small upon variations in the concentration of pendant chains ($B_{2,1}$-$B_{1,5}$-*XX*) but becomes clear if the molecular weights of the pendant chains are below the critical molecular weight needed to obtain entanglement ($B_{2,2}$-$B_{1,1}$-20) or if the molecular weight of the elastic chains is reduced ($B_{2,3}$-$B_{1,5}$-10), giving rise to a more rigid structure.

4. Conclusions

In this work we have applied the DQ NMR technique for probing the influence of pendant chains on model polymer networks with a controlled amount of defects. Small relative variations of average molecular weight between cross-linking points, pendant chain molecular weight, and pendant chain concentration were analyzed. Even for such low concentration of defects DQ NMR appears to be a very sensitive parameter to probe variations of the molecular weight of elastically active chains as well as variations of both the concentration and the molecular weight of pendant chain. The behavior of the NMR parameters was compared with rheological studies of the same polymer networks. An excellent correlation has been found for the $B_{2,1}$-$B_{1,5}$-XX networks in which the pendant chain concentration was increased from 1 to 20 wt % for a fixed length of monofunctional chain (B_1). The influence of variations of the molecular weight of elastically active chains (B_2) on the network structure probed by NMR follows the same trend as the rheological measurements. In addition, the effect of entanglements is clearly depicted in the behavior of both elastic modulus and residual dipolar coupling.

Acknowledgment. We thank the Consejo Nacional de Investigaciones Científicas y Técnicas of Argentina (CONICET), the Agencia Nacional de Promoción Científica y Técnica (ANPCyT), the Secretaría de Ciencia y Técnica of the Universidad Nacional de Córdoba, and the Universidad Nacional del Sur.

References and Notes

(1) Sullivan, J. L.; Mark, J. E.; Hampton, P. G.; Cohen, R. E. *J. Chem. Phys.* **1978**, *68*, 2010−2012.
(2) Andrady, A. L.; Llorente, M. A.; Sharaf, M. A.; Rahalkar, R. R.; Sullivan, J. L.; Falender, J. R. *J. Appl. Polym. Sci.* **1981**, *26*, 1829−1836.
(3) McKenna, G. B.; Gaylord, R. *Polymer* **1988**, *29*, 2027.
(4) Villar, M. A.; Vallés, E. M. *Macromolecules* **1996**, *29*, 4081−4089.
(5) Villar, M. A.; Bibbó, M. A.; Vallés, E. M. *Macromolecules* **1996**, *29*, 4072−4080.
(6) Vega, D. A.; Villar, M. A.; Vallés, E. M.; Steren, C. A.; Monti, G. A. *Macromolecules* **2001**, *34*, 283−288.
(7) Roth, L. E.; Vega, D. A.; Vallés, E. M.; Villar, M. A. *Polymer* **2004**, *45*, 5923−5931.
(8) Vega, D. A.; Gómez, L. R.; Roth, L.; Ressia, J.; Villar, M. A.; Vallés, E. M. *Phys. Rev. Lett.* **2005**, *95*, 166002.
(9) Kluppel, M.; Menge, H.; Schmidt, H.; Schneider, H.; Schuster, R. H. *Macromolecules* **2001**, *34*, 8107−8116.
(10) Schmidt-Rohr, K.; Spiess, H. W. *Multidimensional Solid-State NMR and Polymers*, 2nd printing; Academic Press: London, 1996.
(11) Bovey, F. A.; Mirau, P. A. *NMR of Polymers*; Academic Press: San Diego, 1996.
(12) Simon, G.; Schneider, H. *Makromol Chem., Macromol. Symp.* **1991**, *52*, 233−246. Simon, G.; Baumann, K.; Gronski, W. *Macromolecules* **1992**, *25*, 3624−3628.
(13) Gronski, W.; Hoffmann, V.; Simon, G.; Wutzler, A.; Straube, E. *Rubber Chem. Technol.* **1992**, *65*, 63−77.
(14) Sotta, P.; Fülber, C.; Demco, D. E.; Blümich, B.; Spiess, H. W. *Macromolecules* **1996**, *29*, 6222−6230.
(15) Cohen-Addad, J. P. *Prog. NMR Spectrosc.* **1993**, *25*, 1−316.
(16) Demco, D. E.; Hafner, S.; Fülber, C.; Graf, R.; Spiess, H. W. *J. Chem. Phys.* **1996**, *105*, 11285−11296.
(17) Schneider, M.; Gasper, L.; Demco, D. E.; Blümich, B. *J. Chem. Phys.* **1999**, *111*, 402−415.
(18) Voda, M. A.; Demco, D. E.; Perlo, J.; Orza, R. A.; Blümich, B. *J. Magn. Reson.* **2005**, *172*, 98−109.
(19) Saalwächter, K.; Ziegler, P.; Spyckerelle, O.; Haidar, B.; Vidal, A.; Sommer, J. *J. Chem. Phys.* **2003**, *119*, 3468−3482.
(20) Saalwächter, K. *J. Chem. Phys.* **2004**, *120*, 454−464.
(21) Fechete, R.; Demco, D. E.; Blümich, B. *J. Chem. Phys.* **2003**, *118*, 2411−2421.
(22) Dossin, L. C.; Graessley, W. W. *Macromolecules* **1979**, *12*, 123−130.
(23) Pearson, D. S.; Graessley, W. W. *Macromolecules* **1980**, *13*, 1001−1009.
(24) Ernst, R. R.; Bodenhausen, G.; Wokaun, A. *Principles of Nuclear Magnetic Resonance in One and Two Dimensions*; Clarendon Press: Oxford, 1987.
(25) Cohen-Addad, J. P. *J. Chem. Phys.* **1974**, *60*, 2440−2453.
(26) Urayama, K.; Yokoyama, K.; Kohjiya, S. *Macromolecules* **2001**, *34*, 4513−4518.
(27) Fetters, L. J.; Lohse, D. J.; Richter, D.; Witten, T. A.; Zirkel, A. *Macromolecules* **1994**, *27*, 4639.

MA060011Y